

Tumor-Targeted Delivery of Paclitaxel Using Low Density Lipoprotein-Mimetic Solid Lipid Nanoparticles

Jin-Ho Kim,^{†,‡,#} Youngwook Kim,^{†,#} Ki Hyun Bae,[§] Tae Gwan Park,[§] Jung Hee Lee,^{*,‡,||} and Keunchil Park^{*,†,‡}

[†]Medical Nanoelement Development Center, Samsung Biomedical Research Institute, Seoul 135-710, Republic of Korea

[‡]Department of Health Sciences and Technology, Samsung Advanced Institute for Health Sciences and Technology, Sungkyunkwan University, Seoul 135-710, Republic of Korea

[§]Department of Biological Sciences, Korea Advanced Institute of Science and Technology, Daejeon 305-701, Republic of Korea

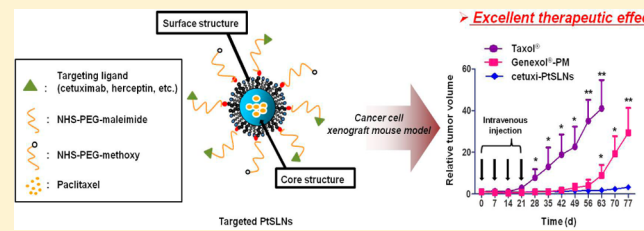
^{||}Department of Radiology, Samsung Medical Center, Sungkyunkwan University School of Medicine, Seoul 135-710, Republic of Korea

[#]Division of Hematology and Oncology, Department of Medicine, Samsung Medical Center, Sungkyunkwan University School of Medicine, Seoul 135-710, Republic of Korea

S Supporting Information

ABSTRACT: Water-insoluble anticancer drugs, including paclitaxel, present severe clinical side effects when administered to patients, primarily associated with the toxicity of reagents used to solubilize the drugs. In efforts to develop alternative formulations of water-insoluble anticancer drugs suitable for intravenous administration, we developed biocompatible anticancer therapeutic solid lipid nanoparticles (SLNs), mimicking the structure and composition of natural particles, low-density lipoproteins (LDLs), for tumor-targeted delivery of paclitaxel. These therapeutic nanoparticles contained water-insoluble paclitaxel in the core with tumor-targeting ligand covalently conjugated on the polyethylene glycol (PEG)-modified surface (targeted PtSLNs). In preclinical human cancer xenograft mouse model studies, the paclitaxel-containing tumor-targeting SLNs exhibited pronounced *in vivo* stability and enhanced biocompatibility. Furthermore, these SLNs had superior antitumor activity to in-class nanoparticulate therapeutics in clinical use (Taxol and Genexol-PM) and yielded long-term complete responses. The *in vivo* targeted antitumor activities of the SLN formulations in a mouse tumor model suggest that LDL-mimetic SLN formulations can be utilized as a biocompatible, tumor-targeting platform for the delivery of various anticancer therapeutics.

KEYWORDS: *cancer therapy, targeted drug delivery system, tumor targeting, paclitaxel, solid lipid nanoparticles*



1. INTRODUCTION

There is widespread expectation that nanotechnology will realize effective cancer treatments and management tools.^{1,2} Nanoparticles are designed engineering products synthesized on a submicrometer scale, and several anticancer therapeutic nanoparticles have been developed to date.^{3–6} A significant number of these nanoparticles, however, often face difficulties in preclinical translation due to inherent toxicity of synthetic materials used in manufacturing nanoparticles.

Biomimetic drug delivery carriers, inspired from abundant pre-existing biosources, thus have great potential for providing safe, biocompatible, and readily applicable delivery vehicles.⁵ Lipid-based nanoparticulate systems have been applied extensively as carriers for the delivery of anticancer drugs because of the better biocompatibility and lower toxicity compared to other materials such as synthetic polymers.^{7–9} In nature, low-density lipoproteins (LDLs) have a core–shell structure comprising a core domain of cholesterol esters and polyunsaturated fatty acids within a lamella-like shell layer of phospholipids, unesterified

cholesterol and a single apolipoprotein, B-100.^{10,11} These LDLs essentially function as 20 nm-sized natural-source nanoparticles that circulate in the human body and transport cholesterol between peripheral tissues. Thus, lipid nanoparticles designed to mimic the composition of LDLs could provide a biocompatible nanoparticulate drug delivery system.

Taxanes, including paclitaxel, are among the most widely used and effective anticancer cytotoxic drugs.^{12,13} However, their poor water solubility presents a pharmaceutical challenge.¹⁴ Taxol, the first clinically available and currently most-used formulation of paclitaxel, is a liquid dissolution of paclitaxel in a 1:1 (v/v) blend of Cremophor-EL and ethanol. It was shown that the Cremophor-EL in Taxol causes severe side-effects, such as hypersensitivity, nephrotoxicity, and neurotoxicity.¹⁵ Thus, there

Received: November 6, 2014

Revised: January 20, 2015

Accepted: February 16, 2015

Published: February 16, 2015

have been numerous attempts to manufacture particulate drug delivery systems of Cremophor-EL-free paclitaxel formulations,^{16–20} and currently, four taxane-based nanoparticle formulations are clinically available. Three of these formulations, nab-paclitaxel (Abraxane), Genexol-PM, and NK105, are nontargeted nanoparticles.^{4,21,22} Prostate-specific membrane antigen (PSMA)-targeting docetaxel-containing nanoparticles (BIND-014) were shown to have high activity in prostate cancer animal model studies and have entered clinical trials.²³

Since lipid nanoparticles are capable of efficiently incorporating small water-insoluble molecules, the development of safe biomimetic drug delivery systems for water-insoluble drugs, such as paclitaxel, can be translated into increased clinical activity and efficient patient care. We recently demonstrated the development of a novel solid lipid nanoparticle (SLN)-based system that mimics a natural-source nanoparticles, LDLs, as a stable and efficient delivery carrier of nucleic acids, including small interfering RNA.²⁴

By modifying the SLNs synthetic process, we here report a successful preclinical translation of a nanosized drug delivery system for paclitaxel as an alternative Cremophor-EL-free formulation. The strong interaction between paclitaxel and the hydrophobic core of the SLNs facilitated efficient loading of paclitaxel into the SLNs. Tumor-targeting ligands, including epidermal growth factor receptor (EGFR)-targeting antibodies, were linked to the surface of the SLN formulations along with a polyethylene glycol (PEG) layer. The *in vitro* and *in vivo* performance of the resulting nanoparticles was characterized extensively, as was their pharmacokinetics, biodistribution, and tolerability. The therapeutic efficacy and biocompatibility of these nanoparticles were tested in multiple mouse cancer models. Finally, the *in vivo* antitumor activity of paclitaxel-containing SLN formulations was compared with the clinically used nanoparticulate formulations of Taxol and Genexol-PM.

2. MATERIALS AND METHODS

2.1. Materials. Paclitaxel (>97%) was obtained from Fluka (Buchs, Switzerland) and used without further purification. Cholestryl oleate, glyceryl trioleate (triolein), cholesterol, fluorescamine, 2-iminothiolane hydrochloride (Traut's reagent, 98%), Sephadryl 200 HOURS, thiazolyl blue tetrazolium bromide (MTT), choursolaminates-T hydrate (98%), and 4,6-diamidino-2-phenylindole (DAPI) were purchased from Sigma-Aldrich (St. Louis, MO, USA). L- α -Dioleoylphosphatidylethanolamine (DOPE) and 3 β -[N-(N',N'-dimethylaminooctane)-carbamoyl] cholesterol hydro-chloride (DC-cholesterol) were provided by Avanti Polar Lipid (Alabaster, AL, USA). Maleimide-poly(ethylene glycol)-succinimidyl carbonate (MAL-PEG-NHS, MW: 5 kDa) and methoxy-poly(ethylene glycol)-succinimidyl carbonate (MeO-PEG-NHS, MW: 5 kDa) were obtained from NOF Corporation (Tokyo, Japan). Green fluorescent Oregon Green 488 paclitaxel was obtained from Molecular Probes (Eugene, OR, USA). PD10 desalting columns were purchased from GE Healthcare U.K. Ltd. (Little Chalfont, Buckinghamshire, U.K.). N-Succinimidyl-3-(4-hydroxyphenyl) propionate (SHPP) was obtained from Thermo Scientific (Rockford, IL, USA). 125 I, at a concentration of 100 mCi/mL, was obtained from PerkinElmer (Waltham, MA, USA). Phosphate buffered saline (PBS), penicillin/streptomycin, fetal bovine serum (FBS), Rosewell Park Memorial Institute 1640 medium (RPMI 1640), and Dulbecco's Modified Eagle's Medium (DMEM) were obtained from Gibco (Grand Island, NY, USA). Genexol-PM was obtained from Samyang Genex

Corporation (Seoul, Korea). Taxol was purchased from Bristol-Myers Squibb (NJ, USA). Cetuximab (MW: 150 kDa) was obtained from Merck KGaA (Darmstadt, Germany), and trastuzumab (herceptin, MW: 150 kDa) was obtained from Roche Pharma (Basel, Switzerland). NCI-H1975, NCI-H1650, NCI-H520, and SK-BR-3 cell lines were purchased from the American Type Culture Collection (VA, USA). PC9 was kindly provided by Dr. K. Nishio (Japan). BALB/c-*nu* mice and C57BL/6 mice were purchased from Orient Bio (Seoul, Korea). Ultrapure water (Millipore, Bedford, MA, USA) was used for all experiments. All other reagents and solvents were of analytic grade.

2.2. Synthesis of tSLNs. Paclitaxel-containing SLNs (tSLNs) for therapeutics were manufactured using a modified solvent-emulsification method. Cholestryl oleate (8.4 mg) and triolein (0.6 mg) as the core structure lipids, and DOPE (5.2 mg), cholesterol (1.8 mg), and DC-cholesterol (10.5 mg) as the surface structure lipids were dissolved in 1.2 mL of a chloroform/methanol mixture (2:1, v/v). Paclitaxel (5 mg) was added to 0.8 mL of the chloroform/methanol mixture (2:1, v/v) and mixed with the previously made lipid solution. Ten milliliters of deionized water was then added, and the mixture was vortexed thoroughly. The suspension was sonicated using a Branson Sonifier 450 (20 kHz, duty cycle = 40, output control = 3.5) for 5 min. The emulsified-solution was transferred to a rotary evaporator, and the solvent was removed by evaporation above 52 °C, which is the melting point of cholestryl oleate. The aqueous dispersion of tSLNs was purified by dialysis (MWCO: 5000) overnight and concentrated up to 5 mg of particle/mL via vacuum evaporation.

2.3. Synthesis of Targeted PtSLNs. Targeting moiety, cetuximab, was conjugated to the tSLNs using the heterobifunctional cross-linking agent, NHS-PEG-maleimide. Briefly, NHS-PEG-maleimide (3 mg) and NHS-PEG-methoxy (6 mg) were dissolved in deionized water at a concentration of 1 mg/mL and added to 1 mL of tSLN solution (5 mg/mL) with vigorous rotation for 12 h at 4 °C to covalently link NHS groups on the NHS-PEG-maleimide or NHS-PEG-methoxy with primary amine groups on the surface of tSLN (molar ratio of 3:1, NHS groups on the PEG/amine groups on the surface of tSLNs). The amount of solvent-accessible amine groups on the tSLN surfaces was quantified using a fluorescamine assay. For the detailed explanation, an amine reactive dye, fluorescamine, was dissolved in acetone at a concentration of 5 mg/mL, and 100 μ L of fluorescamine solution was added to 1 mL of synthesized tSLNs (5 mg/mL) followed by 15 min of incubation. Fluorescence intensity was detected using an automatic microplate reader (Molecular Devices) at an excitation wavelength of 390 nm and an emission wavelength of 475 nm. Glycine (Sigma, MW: 75.07 Da) was used to construct a calibration curve. The resultant PEG-conjugated tSLNs (PtSLNs) were purified using a Sephadryl S-200 column.

Thiolated cetuximab pretreated with Traut's reagent, 2-iminothiolane, was then conjugated to the PtSLNs. Thiolated cetuximab (5 mg, 6 nmol/mg of particles) was incubated with 1 mL of PtSLN (5 mg/mL) at 4 °C overnight (molar ratio of 1:20, thiolated cetuximab/amine groups on the surface of tSLNs). Thioether bond formation between maleimide groups on the PtSLNs and thiol groups on the thiolated cetuximab yielded cetuximab-conjugated PtSLNs (cetuxi-PtSLNs), which were purified using a Sephadryl S-200 column to remove unconjugated cetuximab. For thiolation of cetuximab, cetuximab was modified with Traut's reagent. Four micrograms of Traut's reagent was

dissolved in nitrogen-purged HEPES buffer (pH 8) at a concentration of 1 mg/mL and added to PBS solution containing 1 mg of cetuximab (molar ratio of 5:1, traut's reagent/cetuximab). The mixture was stirred for 2 h at room temperature to allow thioester bond formation. Unreacted materials were removed using a PD-10 gel filtration desalting column. Thiolated cetuximab was concentrated up to 5 mg/mL via vacuum evaporation. The amount of conjugated cetuximab on the PtSLN surfaces was determined using a micro-BCA assay kit (Pierce Biotechnology, IL, USA) using bovine serum albumin (Sigma, MW: 66 500 Da) as a standard.

Other targeting conjugated SLNs moieties, Herceptin-conjugated PtSLNs (hercep-PtSLNs), were also prepared by the protocol described above.

2.4. Characterization of Synthesized SLN Formulations. The hydrodynamic diameters and surface ζ -potential values of the SLN formulations were determined using a Zetasizer nanoseries nano-ZS (Malvern Instruments Ltd., Malvern, U.K.) equipped with a He–Ne laser beam at a wavelength of 663 nm at a fixed scattering angle of 90°. Measurements were conducted in triplicate at 25 °C for all samples appropriately diluted in distilled water.

The size and shape of the SLN formulations were determined using AFM (XE-100, Park systems, Korea). For AFM analysis, 0.1 mL of the SLN formulations (5 mg of particle/mL) were deposited and dried in air on a fresh mica surface and then images were recorded in noncontact mode with an acquisition frequency of 312 kHz.

The amount of paclitaxel loaded within the SLN formulations and paclitaxel release profiles from the SLN formulations were determined using a high performance liquid chromatography (HPLC) system. To a determined amount of paclitaxel loaded within the SLN formulations, 5 mg of freeze-dried tSLNs were solubilized in 20 mL of methanol with shaking for 12 h to extract paclitaxel. After filtration through a Millex SR 0.45 μm filter unit (Millipore Corporation, MA, USA), the amount of paclitaxel in the filtrate was analyzed using a HPLC system equipped with an ACQUITY BEH C18 column (2.1 mm × 100 mm). Acetonitrile was used as the mobile phase with a flow rate of 0.3 mL/min, and eluted peaks were monitored at 227 nm. A calibration curve was obtained using a series of paclitaxel solutions at different concentrations. Results are expressed as the weight/weight percentage of the amount of paclitaxel in the dried SLN formulations.

The *in vitro* release profiles of paclitaxel from the SLN formulations were performed in a PBS solution (pH 7.4) at 37 °C. One milligram of SLN formulations was put in a centrifuge tube and dispersed in 1 mL of PBS solution. The tube was put in an orbital shaker water bath and vibrated at 120 rpm at 37 °C. In a predetermined time, the solution was centrifuged at 11 500 rpm for 15 min, and the supernatants were transferred into a test tube for HPLC analysis. The pellets were redispersed in 1 mL of fresh PBS solution and incubated for continuous release measurements. Released paclitaxel in the supernatants was extracted with 1 mL of methylene chloride and evaporated at room temperature. The dried paclitaxel was dissolved in mobile phase and analyzed by HPLC as described above.

2.5. Cell Culture. The lung cancer cell lines NCI-H1975, NCI-H1650, NCI-H520, and PC9, and the breast cancer cell lines SK-BR-3 were maintained in RPMI 1640 supplemented with 10% (v/v) fetal bovine serum (FBS) and 1% (v/v) antibiotics at 37 °C, 5% CO₂ in a humidified atmosphere.

2.6. Cellular Uptake of SLN Formulations. To compare the cellular uptake of SLN formulations with and without surface modifications, green fluorescent Oregon Green 488 paclitaxel was incorporated into the SLNs instead of paclitaxel. H1975 cells were seeded in 6-well plates at a density of 2×10^4 cells per well and incubated at 37 °C for 24 h, followed by incubation with tSLNs, PtSLNs, or cetuxi-PtSLNs containing fluorescently labeled paclitaxel for 30 min at 37 °C, respectively (25 μg particle/mL). Cellular uptake was stopped by removing the culture medium, and transfected cells were gently washed three times with PBS solution and then dispersed in PBS solution. The fluorescence of the cells was determined using a FACSCalibur Flow Cytometry System (BD bioscience) and CellQuest software (PharMinutestesgen).

To compare the cellular uptake of another targeted SLN formulation, hercep-SLNs, SK-BR-3 cells were seeded in a 6-well plate at a density of 2×10^4 cells per well and incubated at 37 °C for 24 h, followed by incubation with tSLNs, PtSLNs, or hercep-PtSLNs containing fluorescently labeled paclitaxel for 30 min at 37 °C, respectively (25 μg particle/mL).

2.7. Evaluation of Cytotoxic Effect of SLN Formulations. Inhibition of cell growth was determined to evaluate the antitumor efficacy of SLN formulations. H1975 cells were seeded in 96-well plates at a density of 5×10^3 cells per well and grown each at 37 °C for 24 h. The culture medium was then replaced with RPMI 1640 supplemented with 1% (v/v) FBS and 1% (v/v) antibiotics. Cells were incubated with tSLNs, PtSLNs, cetuxi-PtSLNs, or Taxol at a wide range of paclitaxel concentrations from 1 nM to 340 μM . After 48 h of incubation, 10 μL of MTT solution (5 mg/mL) were added to each well. After a 4 h incubation at 37 °C, medium was removed and cells were dissolved in DMSO. The absorbance of each well was measured at 570 nm using an automatic microplate reader (Molecular Devices).

Inhibition of cell growth was also determined by another targeted SLN formulation, hercep-PtSLNs. SK-BR-3 cells were seeded in 96-well plates at a density of 5×10^3 cells per well and grown each at 37 °C for 24 h, and cytotoxicity assay was performed as described above. The percentage growth inhibition was calculated by comparing the average optical density (OD) of control wells with the OD of sample wells as follows:

$$\% \text{ of inhibition} = \frac{\text{OD control wells} - \text{OD sample wells}}{\text{OD control wells}} \times 100$$

2.8. Animal Studies. All animal experiments were done in accordance with a protocol approved by the Institutional Animal Care and Use Committee (IACUC) of Samsung Biomedical Research Institute (SBRI). The SBRI is an Association for Assessment and Accreditation of Laboratory Animal Care International-accredited facility and abides by the Institute of Laboratory Animal Resources (ILAR) guidelines. Female SPF C57BL/6 mice (6–8 weeks old) and BALB/C-nu mice (6–8 weeks old) were housed in a pathogen-free environment.

2.9. Establishment of Xenograft Mouse Models. To generate H1975, H1650, H520, PC9, and SK-BR-3 xenograft mouse models, female SPF BALB/C-nu mice (8 weeks old) were inoculated subcutaneously in the flank region with lung cancer cells (H1975, H1650, H520, or PC9 cells, 5×10^5) or breast cancer cells (SK-BR-3 cells, 5×10^5 cells). When the tumor reached an average volume of 50–100 mm³, treatment was initiated.

2.10. Radiolabeling of SLN Formulations. Radiolabeled tSLNs, PtSLNs, and cetuxi-PtSLNs were prepared using the

Bolton–Hunter method. For the detailed explanation, the Bolton–Hunter reagent, SHPP, was dissolved in DMSO at a concentration of 50 µg/mL, and 10 µL of ¹²⁵I solution (1 mCi) was added to 10 µL of SHPP solution. Chloramine-T was dissolved in PBS solution at a concentration of 10 mg/mL, and 5 µL of Chloramine-T solution was immediately added to the prepared 20 µL of SHPP/¹²⁵I mixture with vigorous mixing for 15 s for iodination of SHPP. Iodinated SHPP solution was extracted with a 1 mL of benzene/DMF mixture (40:1, v/v), and the organic phase was then transferred into a clean tube. The organic solvent was removed by evaporation and dried. Iodinated SHPP was dissolved and reacted in the 1 mL of tSLNs (5 mg/mL) for 2 h at 4 °C to covalently link NHS groups on the iodinated SHPP and primary amine groups on the surface of tSLN surface (molar ratio of 1:10, NHS groups on the SHPP/amine groups on the surface of tSLNs). ¹²⁵I-tSLNs were purified by dialysis (MWCO: 5000) overnight, and subsequent SLNs surface modifications (PtSLNs and cetuxi-PtSLNs) were performed as described in the SLNs synthesis section.

2.11. In Vivo Pharmacokinetic Study of SLN Formulations. Pharmacokinetic (PK) profiles, corrected for radioactive decay to the time of injection, were measured by harvesting blood samples from groups of female SPF C57BL/6 mice. Sampling was performed at specified times after intravenous injection (*i.v.*) injection of 200 µL of ¹²⁵I-tSLNs, ¹²⁵I-PtSLNs, or ¹²⁵I-cetuxi-PtSLNs (5 mg/mL), and the radioactivity of the harvested samples was measured using a γ -counter (1470 automatic Gamma counter, PerkinElmer, USA). The time points used in the experiments were 0.16, 0.32, 0.5, 1, 2, 3, 4, 8, 24, 48, and 72 h, and about 2 µL of blood from the mice tail vein was collected and stored in 8 µL of EDTA solution to prohibit blood coagulation ($n = 6$ mice/time point).

2.12. Tissue Biodistribution of SLN Formulations. To evaluate the *in vivo* tissue biodistribution of the SLN formulations, 200 µL of ¹²⁵I-tSLNs, ¹²⁵I-PtSLNs, and ¹²⁵I-cetuxi-PtSLNs (5 mg/mL) were injected through *i.v.* injection into H1975 tumor-bearing mice. At specific time points (1, 4, and 24 h) after particle injection, mice ($n = 6$ mice/time point) were sacrificed, and samples of tumor and organs were harvested and weighed. The injected dose per gram tissue (%ID/g) was calculated from the radioactivity measured using a γ -counter.

2.13. Determination of the Tolerable Dose of SLN Formulations. The effectively tolerable dose (eTD: defined as the dose at which experimental animals are able to tolerate with *in vivo* anticancer efficacy, but still below maximum tolerable dose) for systemically administered cetuxi-PtSLNs was determined in healthy female C57BL/6 mice. The mice received *i.v.* injection of 100, 200, or 400 mg of particles/kg of cetuxi-PtSLNs, or PBS solution as a control through the tail vein for 4 consecutive days ($n = 4$ for each group). The health of the animals was closely monitored, including loss of consciousness after treatment or body weight changes.

2.14. In Vivo Antitumor Efficacy of SLN Formulations. *In vivo* tumor growth inhibition was performed to evaluate the antitumor efficacy of SLN formulations. Female SPF BALB/C-nu mice bearing H1975, H1650, H520, or PC9 tumors were randomly divided into 5 groups ($n = 9$ mice/group), and tSLNs, PtSLNs, cetuxi-PtSLNs, cetuxi-PSLN (vehicle), or PBS solution was administrated intravenously at 22 mg of paclitaxel/kg once a week for 3 weeks. Tumor size was monitored with calipers once a week for 6 weeks, and tumor volume was calculated according to the formula

$$V = \frac{1}{2} \text{smaller diameter} \times (\text{larger diameter})^2$$

We continuously studied the antitumor efficacy of SLNs formulations that bear another tumor-targeting ligand, herceptin. Female SPF BALB/C-nu mice bearing SK-BR-3 tumors were randomly divided into 3 groups ($n = 9$ mice/group), and PtSLNs, hercep-PtSLNs, or PBS solution was administrated intravenously at 22 mg of paclitaxel/kg once a week for 3 weeks. Tumor size was monitored with calipers once a week for 7 weeks, and tumor volume was calculated as described above.

We also studied the antitumor efficacy of cetuxi-PtSLNs in comparison with the conventionally used paclitaxel-delivering formulations, Taxol and Genexol-PM. Female SPF BALB/C-nu mice bearing H1975 or H1650 tumors were randomly divided into 3 groups ($n = 6$ mice/group), and cetuxi-PtSLNs at their effectively tolerated dose (eTD, 22 mg of paclitaxel/kg) and Taxol and Genexol-PM at their maximally tolerable dose (MTD, Taxol, 20 mg of paclitaxel/kg; Genexol-PM, 60 mg of paclitaxel/kg) were administered intravenously once a week for 3 weeks. Tumor size was monitored with calipers once a week for 11 weeks, and tumor volume was calculated as described above.

The antitumor effect of cetuxi-PtSLNs was further evaluated by determining dose-dependent tumor growth inhibition. Female SPF BALB/C-nu mice bearing H1975 tumor were randomly divided into 6 groups ($n = 6$ mice/group) and received *i.v.* injections of 1.1, 2.2, 5.5, 12, and 22 mg of paclitaxel/kg and PBS solution once a week for 2 weeks. Tumor size was monitored with calipers once a week for 3 weeks, and tumor volume was calculated as described above.

2.15. In Vivo Intracellular Delivery of Paclitaxel. Excised tumor tissues were examined histologically to determine intracellular uptake of nanoparticle-delivered paclitaxel. To visualize the intracellular uptake of paclitaxel *in vivo*, green fluorescent Oregon Green 488 paclitaxel incorporating SLN formulations were used. Female SPF BALB/C-nu mice bearing H1975 tumor received a single intravenous administration of PtSLNs, cetuxi-PtSLNs, or fluorescently labeled paclitaxel at an equivalent paclitaxel concentration of 22 mg of paclitaxel/kg. One day after treatment, tumor tissues were excised, fixed, paraffin-embedded, and sectioned into 10 µm thick slices. Paraffinized tumor sections were dewaxed in xylene, passaged through graded alcohols, and rinsed in distilled water. After deparaffinization, the cell nuclei were stained with DAPI (1.5 µg/mL in PBS solution) for 10 min. The green fluorescence signal was monitored using a LSM700 confocal laser-scanning microscope (Carl Zeiss, Germany).

2.16. Apoptosis Assay. The terminal deoxynucleotidyl transferase-mediated dUTP nick-end labeling (TUNEL) assay was performed to detect targeted-SLNs induced apoptosis using an *in situ* cell detection kit (TAKARA BIO Inc. Japan). Female SPF BALB/C-nu mice bearing H1975 tumor received a single dose of Taxol or cetuxi-PtSLNs at 22 mg of paclitaxel/kg intravenously. One day (for Taxol and cetuxi-PtSLNs) or 7 days (for cetuxi-PtSLNs) after injection, tumors were harvested and fixed in 4% paraformaldehyde solution. Tumor tissues were paraffin-embedded and then sectioned into 10 µm thick slices. Paraffinized tumor sections were dewaxed in xylene, passaged through graded alcohols, and rinsed in distilled water. Tumor sections were treated with 1 mL of proteinase K (100 µg/mL) for 10 min at room temperature and washed with PBS solution. Sections were then treated with 50 µL of labeling reaction mixture that consisted of 5 µL of TDT enzyme and 45 µL of

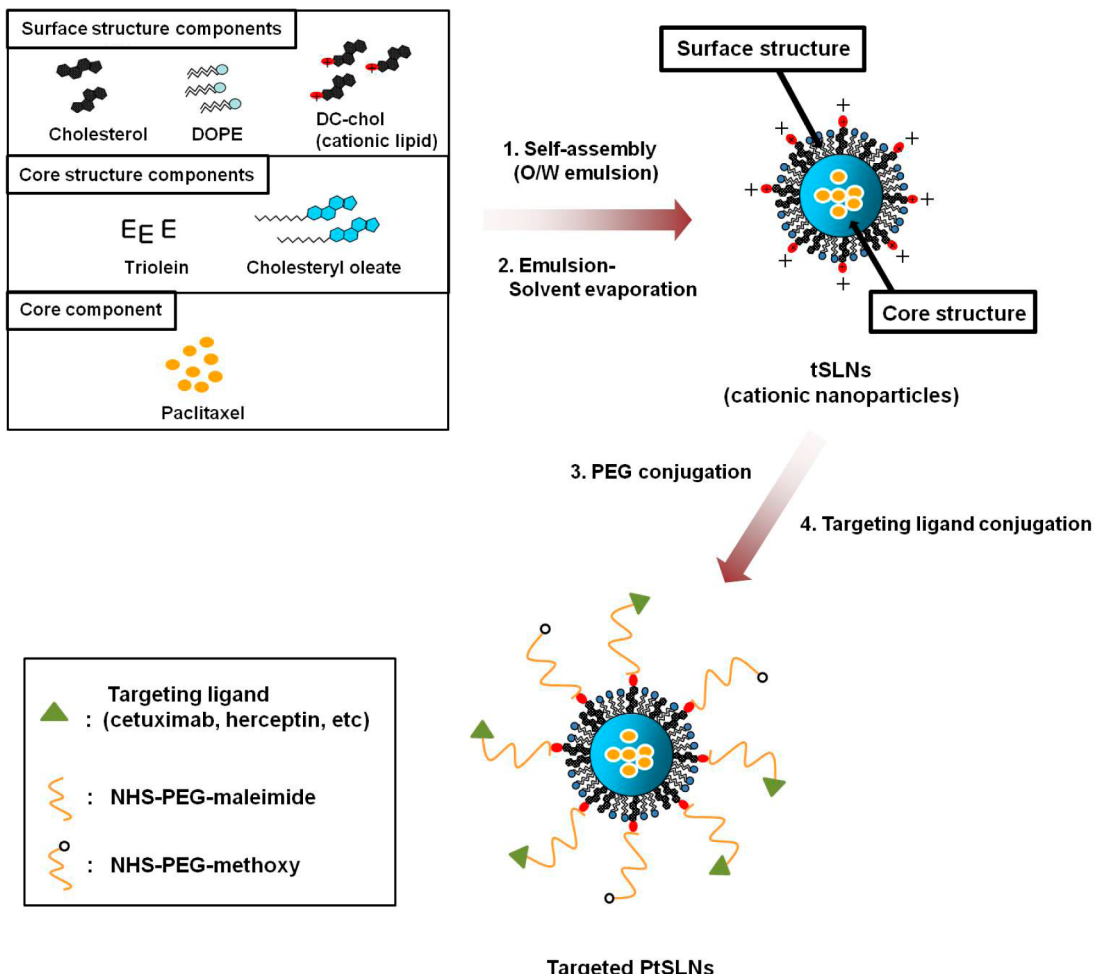


Figure 1. Schematic illustration of targeted PtSLNs. SLNs were synthesized by self-assembly of the specified constituents. Shown right and below are the synthetic steps used to prepare targeted PtSLNs. + signs on the surface of the schematic representation of the particle indicate positively charged amine groups from DC-cholesterol.

labeling-safe buffer at the volume ratio of 1:9 in a 37 °C humidified chamber for 60–90 min. The reaction was terminated by washing the tumor sections 3 times with PBS solution for 5 min per wash. After washing with PBS solution, the cell nuclei were stained with DAPI (1.5 µg/mL in PBS solution) for 10 min. The fluorescence signals from apoptotic cells were examined using a LSM700 confocal laser-scanning microscope.

2.17. Statistical Analysis. Quantitative data are expressed as means \pm standard deviations, unless otherwise indicated. Statistical comparisons were made using Student's *t*-test for two groups, and one-way ANOVA for multiple groups. Probability (*P*) values <0.05, 0.01, or <0.001 were considered statistically significant.

3. RESULTS AND DISCUSSION

3.1. Synthesis and Characterization of SLN Formulations. The tumor-targeted, PEGylated, paclitaxel-containing SLNs (targeted PtSLNs) are composites of nanosized lipid micellar particles that contain paclitaxel in the core region surrounded by a protective PEG layer with tumor-targeting ligands (Figure 1).

We used LDL-mimicking SLNs that we developed in a previous study as the backbone of the particle design.²⁴ The SLNs formed a lipid micelle structure composed of a hydrophobic core containing paclitaxel and amphiphilic surface

layers attached to targeting ligands (Figure 1; Figure S1 and Table S1 in the Supporting Information). PEG derivatives were covalently attached to surface amine groups to provide the SLNs with *in vivo* compatibility and immune-evasive properties. Finally, tumor-targeting ligands, including antibodies, were conjugated to the distal ends of the PEG molecules to enhance the particles' tumor-targeting efficacy.

To synthesize targeted PtSLNs, three different sequential formulations of nanoparticles were prepared: (1) non-PEGylated paclitaxel-containing SLNs without a targeting ligand (tSLNs), (2) PEGylated paclitaxel-containing SLNs without a targeting ligand (PtSLNs), and (3) targeted and PEGylated paclitaxel-containing SLNs (targeted PtSLNs) (Figure 1).

To manufacture targeted PtSLNs, we initially used an EGFR-targeting antibody, cetuximab, as the tumor-targeting ligand. We set up reaction so that all the amine groups on the surface of tSLNs were virtually substituted by PEG derivatives (Figure S2 in the Supporting Information). We then determined the amount of cetuximab (6 nmol/mg of particles, Figure S3 in the Supporting Information) that leads to the maximum efficacy of cell internalization of targeted nanoparticles.

The prepared SLN formulations were then physicochemically characterized. The amount of paclitaxel encapsulated within the tSLNs, determined by high performance liquid chromatography (HPLC) analysis, was $11 \pm 0.8\%$ (w/w). The total paclitaxel

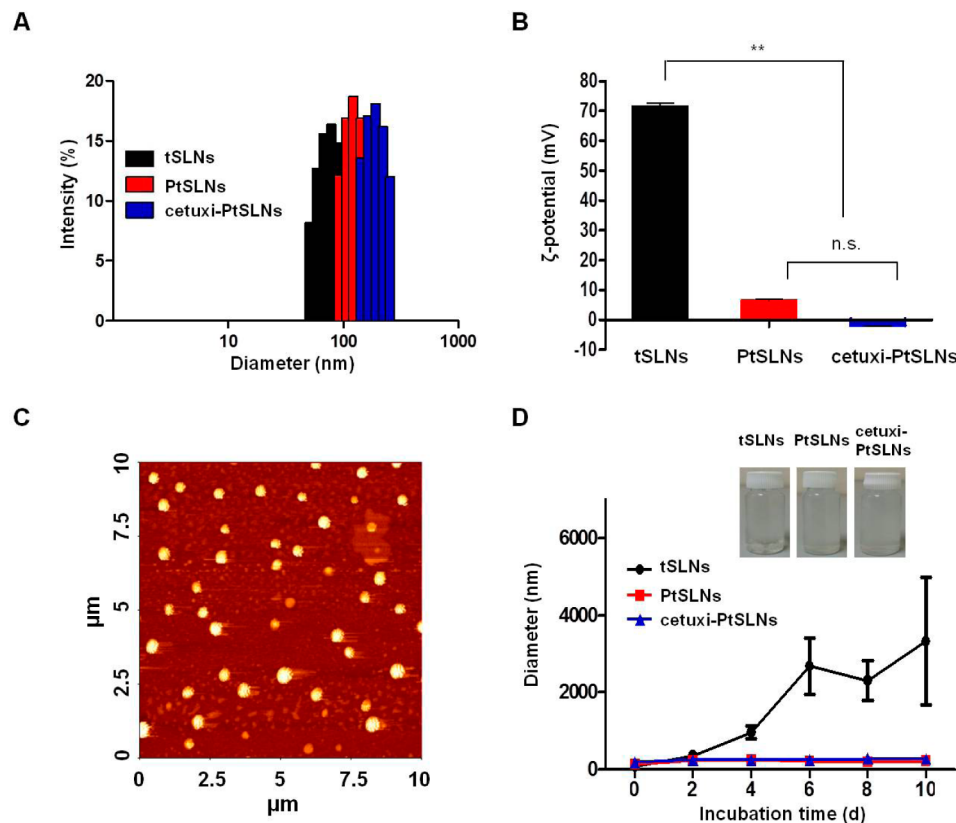


Figure 2. Physicochemical properties of SLN formulations. (A,B) Hydrodynamic diameters and ζ -potential values of SLN formulations in deionized water. (C) AFM image of cetuxi-PtSLNs. Synthesized cetuxi-PtSLNs were visualized using AFM to determine the physical appearance of the nanoparticles. (D) Time course changes of the hydrodynamic diameter of SLN formulations in PBS solution (pH 7.4) containing 10% FBS (v/v). The concentration of the SLN formulations was 5 mg/mL. Data presented are average \pm SD. Statistically significant differences are marked as ** p < 0.01 and n.s., not significant (n = 3 independent measurements).

loading amount ($550 \pm 40 \mu\text{g}/\text{mL}$) at 5.0 mg/mL of tSLNs was significantly higher than the solubility of paclitaxel in water ($<1 \mu\text{g}/\text{mL}$). By dynamic light scattering (DLS), the mean diameter of the tSLNs was measured as $85.8 \pm 1.6 \text{ nm}$, with a surface charge value of $71.3 \pm 2.1 \text{ mV}$. In comparison, cetuxi-PtSLNs had an average hydrodynamic diameter of $160.4 \pm 0.9 \text{ nm}$, with a surface charge value of $-1.3 \pm 1.0 \text{ mV}$ (Figure 2A,B; Table S2 in the Supporting Information). Incorporation of PEG (and cetuximab) increased the particle size and changed the surface charge from positive to near-neutral. Similarly to cetuxi-PtSLNs, herceptin conjugated PtSLNs showed average hydrodynamic diameter of $168.2 \pm 1.5 \text{ nm}$, with a surface charge value of $-0.8 \pm 1.7 \text{ mV}$. To confirm that nanoparticles were homogeneously synthesized, the physical appearance of the cetuxi-PtSLNs was visualized by atomic force microscopy (AFM), which revealed that the targeted PtSLNs had a spherical shape with virtual monodispersity and an apparent physical diameter consistent with that obtained from DLS methods (Figure 2C). Dispersion stability of SLN formulations was markedly improved with the attachment of PEG on the surface. *In vitro* incubation of tSLNs in the presence of 10% serum resulted in aggregate formation, whereas the PEGylated version of SLN formulations (PtSLN and cetuxi-PtSLNs) remained stable for several days under the same conditions (Figure 2D; Figure S4 in the Supporting Information).

3.2. Paclitaxel Delivery Efficiency and Therapeutic Efficacy of SLN Formulations *In Vitro*. We anticipated that the presence of targeting ligands and PEG moieties on the surface of the targeted PtSLNs would have a measurable effect on

the nanoparticles' ability to target cancer cells. To follow the fate of nanoparticles and to determine the effects of conjugating PEG and tumor-targeting ligands on the cellular uptake of the nanoparticles, we prepared green-fluorescent paclitaxel-loaded SLN formulations with or without PEG and targeting ligands. These particle preparations were added to the culture medium of human lung cancer cells, H1975, that overexpress EGFR protein. The analysis of the extent and proportion of nanoparticles uptake showed that, compared to tSLNs, the uptake of PtSLNs was significantly hampered by the presence of a superficial PEG layer. In contrast, both the proportion of cells that took up nanoparticles and the amount of nanoparticles taken up per cell were dramatically increased by the presence of the EGFR-targeting ligand, cetuximab (Figure 3).

To illustrate whether increased cellular uptake of nanoparticles due to the presence of cancer cell-targeting antibodies on the nanoparticles translated into increased therapeutic efficacy, we determined the *in vitro* cytotoxicity profiles of the nanoparticles in H1975 cancer cells. As shown in Figure 4A and Table S3 in the Supporting Information, the presence of tumor-targeting antibodies markedly increased the efficacy of drug delivery to cancer cells cultured *in vitro*.

To determine the biocompatibility of SLNs as a drug delivery vehicle, we prepared SLN formulations without paclitaxel (Figure 4B). When cells were treated with SLNs, PSLNs, cetuxi-PSLNs (all without paclitaxel), or a mixture of Cremophor-EL/ethanol at concentrations containing equivalent amounts of paclitaxel, no SLN formulations without paclitaxel exhibited antiproliferative activity. However, a mixture of

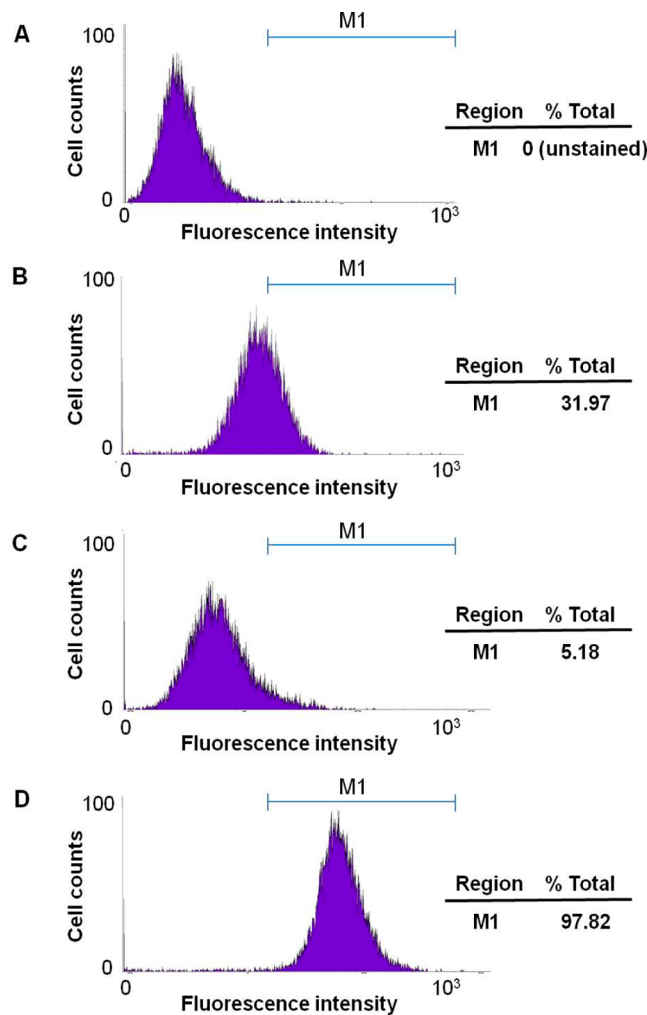


Figure 3. Targeted delivery of cetuxi-PtSLNs in cultured cell experiments. Flow cytometric analysis of H1975 cells following incubation with (A) nontreated control, (B) tSLNs containing Oregon Green 488 paclitaxel, (C) PtSLNs containing Oregon Green 488 paclitaxel, and (D) cetuxi-PtSLNs containing Oregon Green 488 paclitaxel at equivalent SLNs concentration of 25 μ g of particle/mL for 30 min at 37 °C, respectively.

Cremophor-EL/ethanol, which is practically a control Taxol containing no paclitaxel, showed significant cytotoxicity because of the nonspecific toxicity caused by the organic solvents (Figure 4B).

The modular nature of the nanoparticle synthesis enables alternative targeting moieties to be incorporated, resulting in the ability to manufacture nanoparticles targetable to other types of cancer cells. As a proof of concept, we conjugated a Her2-targeting antibody, trastuzumab (herceptin), to the surface of nanoparticles to generate hercep-PtSLNs. As was the case for cetuxi-PtSLNs, the intracellular delivery of paclitaxel by hercep-PtSLNs to human breast cancer cells, SK-BR3, overexpressing the Her2 protein was markedly enhanced due to the presence of cancer cell-targeting antibodies, and this effect was translated into increased therapeutic efficacy (Figures S5 and S6 and Table S3 in the Supporting Information).

3.3. Pharmacokinetics and Tissue Distribution of SLN Formulations.

To monitor the effect of incubating SLN formulations under physiological conditions, we first measured *in vitro* drug release profiles of tSLN, PtSLN, and cetuxi-PtSLN (Figure 5A) in a PBS solution (pH 7.4) at 37 °C. The incorporated paclitaxel was released in a sustained manner over 24 h without a significant initial burst. Paclitaxel release from the cetuxi-PtSLNs was relatively slower compared to that from the PtSLN or tSLN, possibly because the paclitaxel took longer to diffuse from the larger micelles into the medium.

Next, pharmacokinetic (PK) profiles of SLN formulations were obtained by systemic intravenous administration of radiolabeled nanoparticles into mice (Figure 5B). tSLNs were cleared rapidly from systemic circulation following intravenous administration. In contrast, PtSLNs had good *in vivo* stability. The presence of cancer-targeting moieties at the distal end of the PEG molecules did not interfere with the stability or PK of the SLNs, and PEGylation helped to stabilize the *in vivo* behavior of the tumor-targeting PtSLNs (Figure 5B). Consequently, PtSLNs and targeted PtSLNs had a significantly longer circulation time than tSLNs (Table S4 in the Supporting Information). A conservative estimate of the preterminal phase disposition half-life of cetuxi-PtSLNs was 40.68 h, indicating prolonged paclitaxel availability in systemic circulation (Table S4 in the Supporting Information).

After a single dose injection of one of three different SLN formulations, mice were sacrificed 1, 4, or 24 h after injection to

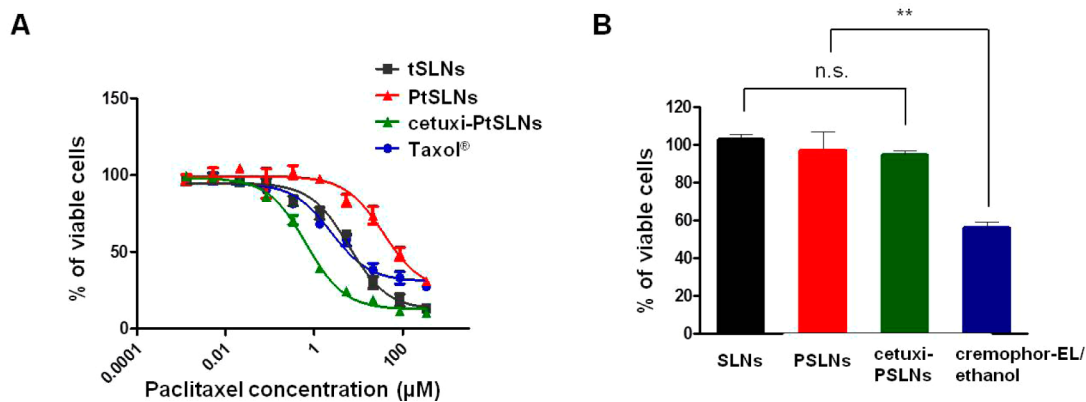


Figure 4. Cell viability assay of the SLN formulations. (A) Cell viability assay of tSLNs, PtSLNs, cetuxi-PtSLNs, and Taxol in H1975 cells after 48 h incubation at varying concentrations of paclitaxel. (B) The viability of cells treated with paclitaxel-free vehicles was shown at an equivalent paclitaxel concentration of 5 μ M. Data presented are average \pm SD. Statistically significant differences are marked as ** p < 0.01 and n.s., not significant (n = 3 independent measurements).

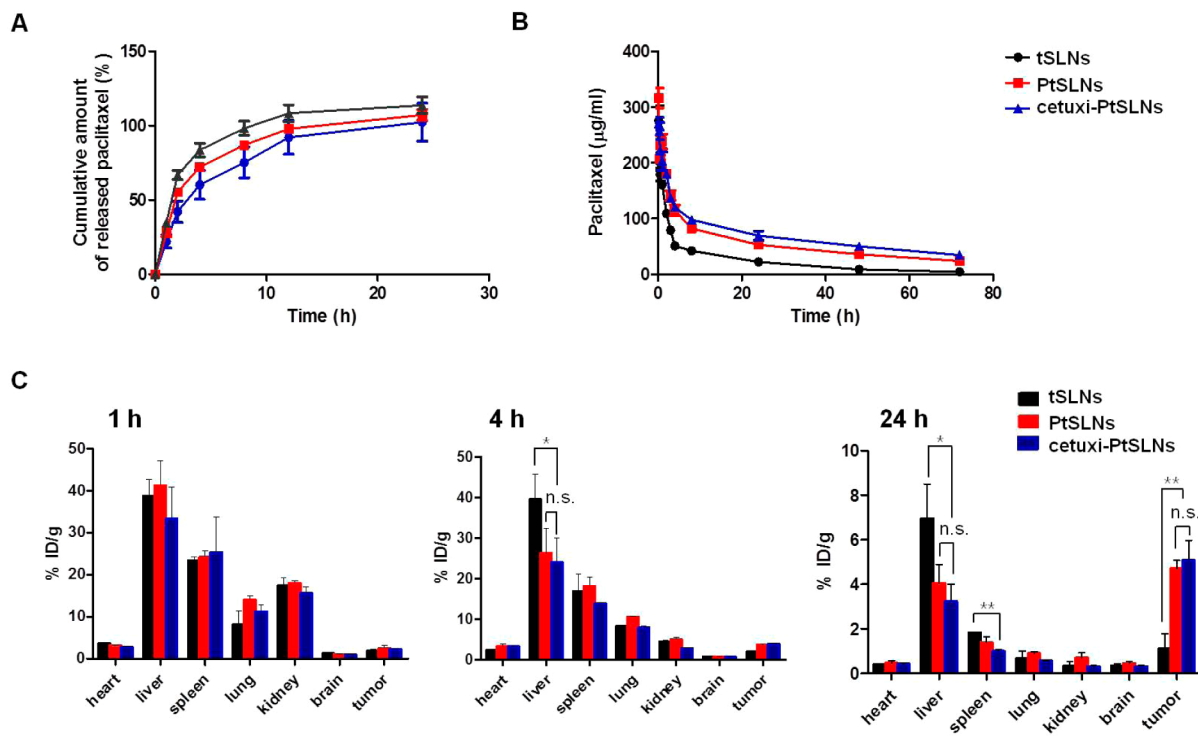


Figure 5. *In vitro* paclitaxel release, PK, and tissue biodistribution of SLN formulations. (A) *In vitro* release profiles of paclitaxel from tSLNs, PtSLNs, and cetuxi-PtSLNs in PBS solution (pH 7.4). (B) PK profiles of the SLN formulations. Following intravenous administration of ^{125}I -tSLNs, ^{125}I -PtSLNs, or ^{125}I -cetuxi-PtSLNs to C57BL/6 mice, serial blood samples were collected from each animal at various times, and total paclitaxel blood concentrations were analyzed. Data represent mean \pm SD ($n = 6$). (C) Tissue biodistribution of the SLN formulations. Two hundred microliter (5 mg particle/mL) aliquots of ^{125}I -tSLNs, ^{125}I -PtSLNs, or ^{125}I -cetuxi-PtSLNs were administered intravenously to nude mice bearing H1975 tumors. The tissue biodistribution was evaluated 1, 4, and 24 h after administration. Statistically significant differences are marked as * $p < 0.05$, ** $p < 0.01$, and n.s., not significant, respectively ($n = 6$).

examine the tissue distribution of the nanoparticles (Figure 5C). The primary site of early phase nanoparticles accumulation was found to be liver, and the concentration of nanoparticles in the liver was in the order of tSLNs > PtSLNs \approx cetuxi-PtSLNs. At all time points, the amount of nanoparticles measured in the tumors of mice followed the order of cetuxi-PtSLNs \approx PtSLNs > tSLNs. Specifically, 24 h after administration, the radiolabeled nanoparticle level in tumors treated with cetuxi-PtSLNs was $5.06 \pm 0.89\% \text{ ID/g}$, which was 4.6-fold higher than that in the tSLN-treated tumors ($p < 0.01$). In contrast, the difference in radioactivity between tumors treated with targeted PtSLNs and PtSLNs (without targeting ligands) was not significant, demonstrating that these two classes of nanoparticles accumulate similarly at the macro-organ level.

3.4. Antitumor Activity of SLN Formulations in Preclinical Animal Model Studies. We first conducted *in vivo* dose-escalating studies, which led to the designation of the effectively tolerated dose (eTD) of targeted PtSLNs as 200 mg of particles/kg (22 mg of equivalent dose of paclitaxel/kg) for subsequent *in vivo* experiments (Figure S7 in the Supporting Information).

We then evaluated the *in vivo* antitumor activity of cetuxi-PtSLNs in mice bearing EGFR protein-overexpressing NCI-H1975, NCI-H1650, NCI-H520, or PC9 lung cancer cell xenografts. Mice were treated with the effectively tolerated dose (eTD: 22 mg of paclitaxel/kg) of cetuxi-PtSLNs once a week for 3 weeks. For comparison, equivalent doses of tSLNs, PtSLNs, or cetuxi-PtSLNs (vehicle) were injected on the same schedule as cetuxi-PtSLNs. Treatment of mice bearing H1975 tumors with cetuxi-PtSLNs resulted in marked tumor shrinkage,

with several mice maintaining a near-complete response 3 weeks after the final drug injection (Figure 6A). Moreover, we found that the antitumor effect of cetuxi-PtSLNs was robustly reproducible in mice with tumors seeded by one of three other lung cancer cell types expressing EGFR protein (Figure 6B–D). By the end of the observation period, the tumors of cetuxi-PtSLN-treated mice were nonobservable or notably smaller than those of the other groups (Figure 6).

To demonstrate that PtSLNs bearing other tumor-targeting ligands have equally effective antitumor activity, we changed the targeting moiety from cetuximab to the Her2-targeting antibody, herceptin. When hercep-PtSLNs were directly tested *in vivo* in mice with Her2-overexpressing breast cancer cell xenograft, SK-BR-3, they showed markedly enhanced therapeutic activity relative to control nanoparticles (Figure 7A).

To evaluate the antitumor efficacy of cetuxi-PtSLNs in a clinically relevant setting, we compared its therapeutic effects directly with those of Taxol, which is a Cremophor EL-solubilized form of paclitaxel, or with Genexol-PM, which is paclitaxel-based nanoparticles approved for clinical use. The maximally tolerable dose (MTD, therapeutic dose established by mouse studies) for each drug¹⁶ or eTD for cetuxi-PtSLNs was administered to mice once a week for 3 weeks, and the tumor volumes of each treatment group were recorded for an additional 8 weeks. While drugs were being administered, there were no obvious differences in tumor volume among the three treatment arms. When drug treatment was stopped after 3 weeks, however, tumor responses began to dichotomize: the volume of tumors in the Taxol-treated group started to increase rapidly upon drug withdrawal (Figure 7B). Four weeks after the final administration

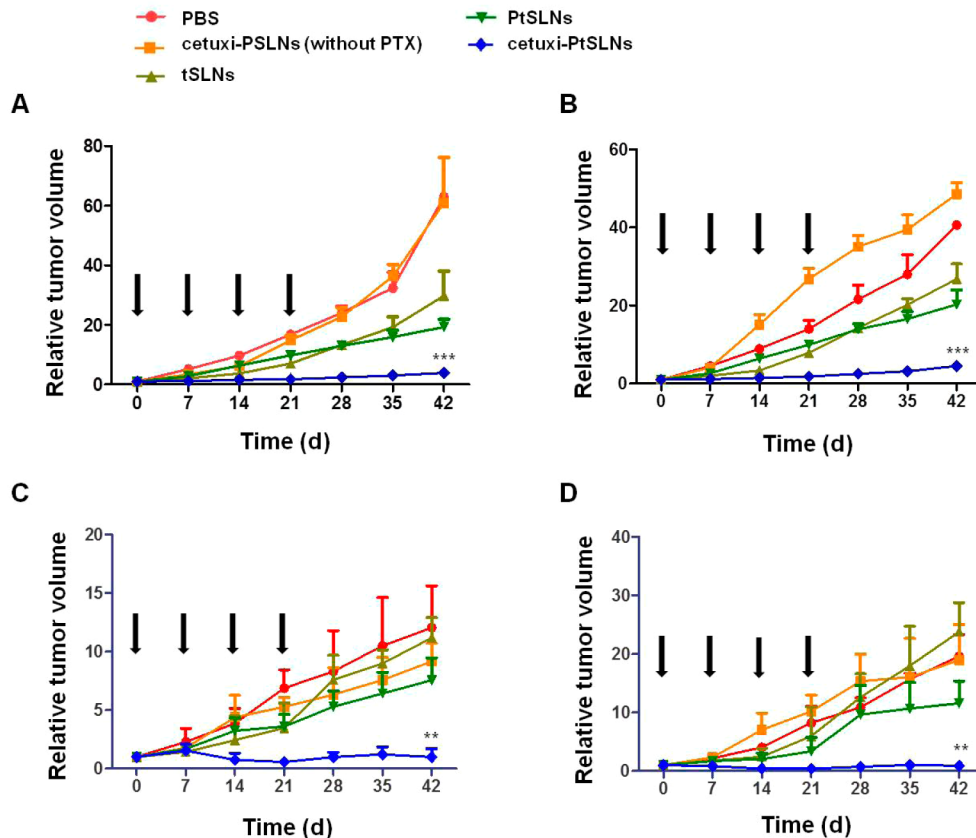


Figure 6. *In vivo* antitumor effect of SLN formulations. Tumor growth curves for nude mice bearing (A) H1975, (B) H1650, (C) H520, and (D) PC9 tumors were recorded after intravenous administration of SLN formulations at the dose of 22 mg of paclitaxel/kg. All solid arrows indicate the time point of intravenous administrations of the therapeutic, and all data are shown as means \pm SD. Statistically significant differences with PtSLNs group are marked as $^{**}p < 0.01$ and $^{***}p < 0.001$, respectively ($n = 9$ for each group).

of drugs, the tumor volume of Genexol-PM-treated mice started increasing, and by 11 weeks, the tumor volumes of cetuxi-PtSLN-treated mice were significantly smaller than those of Genexol-PM or Taxol-treated mice (Figure 7B).

Delayed tumor growth and robust antitumor responses were also observed in mouse groups that received cetuxi-PtSLNs at doses of 2.2, 5.5, and 11 mg of paclitaxel/kg, well below their eTD of 22 mg of paclitaxel/kg (Figure S8 in the Supporting Information). These results demonstrated that cetuxi-PtSLNs have excellent antitumor activity over a wider range of therapeutic concentrations (2.2–22 mg of paclitaxel/kg in mice). This also demonstrated that the subthreshold level of cetuxi-PtSLNs was more effective than Taxol (Table S5 in the Supporting Information) at its MTD.

The PK experiments showed that PEGylation of nanoparticles resulted in enhanced *in vivo* stability, which translated into preferential accumulation in tumor tissues. The therapeutic efficacy of targeted PtSLNs, however, was far superior to that of nontargeted PtSLNs. To investigate whether the enhanced tumocidal activity of targeted PtSLNs was due to increased intracellular delivery of paclitaxel to cancer cells, mediated by the presence of cancer-targeting ligands, we injected green-fluorescent paclitaxel-containing PtSLNs or targeted PtSLNs into tumor-bearing mice. Confocal imaging of tumor sections 1 day after a single drug injection revealed robust intracellular accumulation of fluorescent signals in cancer cells of mice treated with targeted PtSLNs compared with nontargeted PtSLNs (Figure 8). Moreover, the green fluorescent signal was

widespread throughout the cancer tissue sections, indicating that therapeutic delivery to cancer tissue was fairly homogeneous within a 24 h time frame. Strong TUNEL-positive signals were detected in tumor sections from mice injected with targeted PtSLNs, indicating apoptotic tumor cell death (Figure 9). The degree of TUNEL-positive staining correlated well with macroscopic tumor responses. Moreover, the TUNEL-positive cells in tumor sections were clearly detectable on day 7 after a single-dose injection of targeted PtSLNs (Figure 9C).

4. CONCLUSION

In the present study, we have demonstrated that SLNs with an LDL-mimicking composition and components can be used as efficient nanoscale particulate drug delivery systems for the targeted delivery of paclitaxel molecules.

We have shown a new approach to nanoparticle development and introduced physicochemical diversity in the nanoparticle design, while optimizing the nanoparticle engineering to a clinically validated set of biomaterials. This approach consisted of evaluation of a combinatorial SLN formulations library, which varied systematically with respect to parameters (size, surface charge, targeting ligand density, drug loading, and drug release) that affect PK profile, tissue biodistribution, intracellular drug delivery, and efficacy of the encapsulated therapeutic agent. The resultant optimized SLN formulations (targeted PtSLNs) performed better than currently available clinical-grade taxane-based nanoparticles.

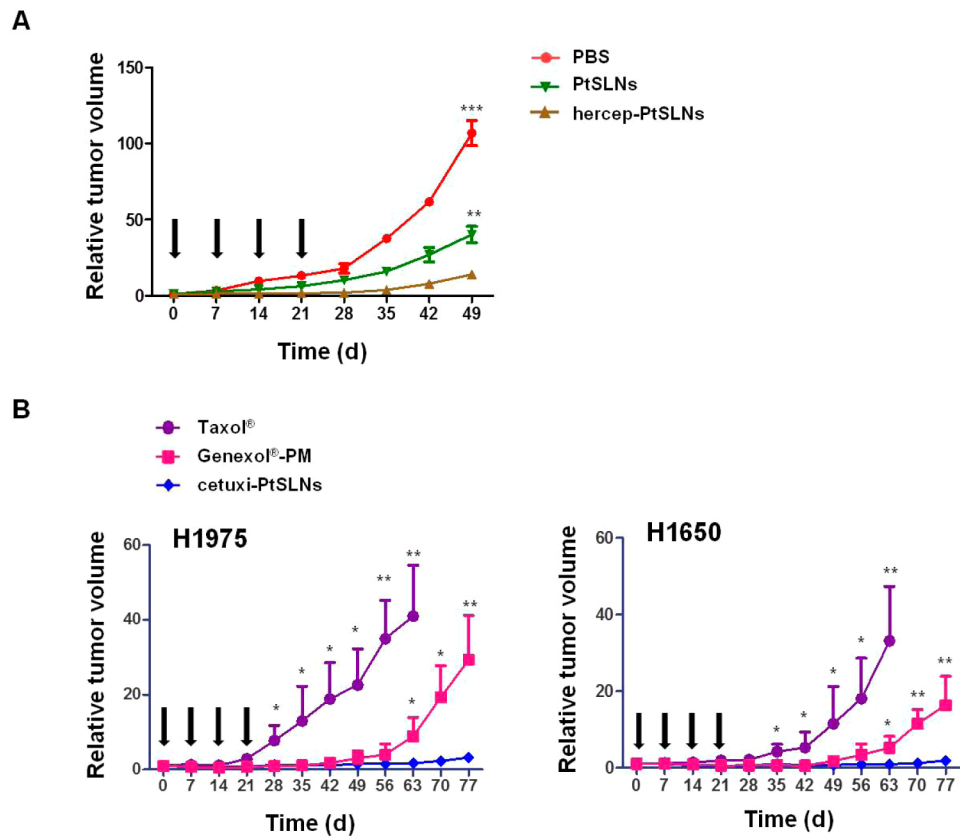


Figure 7. Utilizing as tumor-specific therapeutic carriers for treating various cancer types and comparison of cetuxi-PtSLNs with in-class paclitaxel-based clinical therapeutics. (A) Tumor growth curves of nude mice bearing SK-BR-3 tumors were recorded after intravenous administration of hercep-PtSLNs or control formulations at the dose of 22 mg of paclitaxel/kg. All solid arrows indicate the time point of intravenous administration of the therapeutic, and all data are shown as mean \pm SD. Statistically significant differences with hercep-PtSLNs group are marked as ** $p < 0.01$ and *** $p < 0.001$, respectively ($n = 9$ for each group). (B) Tumor growth curves of nude mice bearing H1975 or H1650 tumors were recorded after intravenous administration of cetuxi-PtSLNs, Taxol, or Genexol-PM at their eTD or MTD (cetuxi-PtSLNs, 22 mg of paclitaxel/kg; Taxol, 20 mg of paclitaxel/kg; Genexol-PM, 60 mg of paclitaxel/kg). All solid arrows indicate the time point of intravenous administrations of the therapeutic, and all data are shown as means \pm SD. Statistically significant differences with cetuxi-PtSLNs group are marked as * $p < 0.05$ and ** $p < 0.01$, respectively ($n = 6$ for each group).

The similarity in PK profile and tissue biodistribution at the tumor site of targeted vs nontargeted PEGylated SLNs suggests that pericellular nanoparticles presented in the cancerous tissue are more readily taken up by cancer cells when nanoparticles are coated with cancer-cell specific targeting molecules. The relationship between tumor-targeting ligands and the efficiency of particle uptake has been evaluated in several studies,^{25–28} all of which have demonstrated that targeted nanoparticles deliver a higher payload into target cancer cells than their nontargeting counterparts.

In our *in vivo* animal model studies, tumor-targeting PtSLNs robustly outperformed clinically approved paclitaxel formulation, Taxol. The prolonged efficacy of tumor-targeting PtSLNs compared with Taxol can be attributed to multiple factors, including the enhanced *in vivo* stability of the tumor-targeting PtSLNs and the consequent maintenance of effective systemic therapeutic concentrations. It is known that free molecular paclitaxel is rapidly cleared from the systemic circulation,²⁹ whereas tumor-targeting PtSLNs have a terminal-phase blood half-life longer than 40 h. This increased half-life of the tumor-targeting PtSLNs likely contributed to the enhanced availability of payload molecules circulating in the blood, which in turn translated into increased accumulation of the therapeutic drug in target tissues over a prolonged period of time. The half-life of targeted PtSLNs is longer than that reported for BIND-014,

another clinical-stage tumor-targeting docetaxel-based nanoparticle.²³ Although studies have demonstrated constant exponential clearance of BIND-014 from systemic circulation, it is nonetheless rapidly cleared from the systemic circulation, with about 1% of the injected dose remaining at 24 h. In contrast, approximately 20% of the targeted PtSLNs were still present in circulation at 24 h. It is also of note that targeted PtSLNs had more potent antitumor activity than Genexol-PM, a paclitaxel-based polymeric micelle approved for clinical use.¹⁶

The apoptotic activity of targeted PtSLNs was robustly detectable 7 days after a single injection of the targeted nanoparticles. Because apoptotic cells are cleared rapidly from cancer fields within 1 day, the presence of TUNEL-positive cancer cells several days after the injection of targeted PtSLNs suggests that cell death activity was continuously ongoing and that anticancer therapeutics were constantly being supplied to the cancer field. In contrast, this efficient and prolonged induction of apoptosis was not visible when the free molecular form of paclitaxel, Taxol, was administered. Thus, prolonged efficacy due to the enhanced stability of the drug carrier clearly contributed to the enhanced dispersal of targeted PtSLNs in cancerous tissue, and the targeting ligands enabled efficient delivery of the therapeutic payload as well as consequent induction of cancer cell death. These results indicate that appropriate combinations of targeting agents and therapeutic

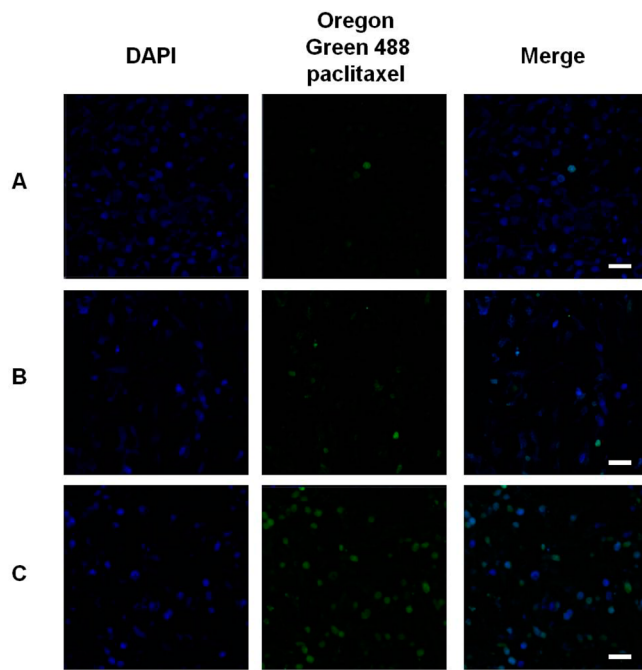


Figure 8. Confocal microscopic observations of intracellular delivery of paclitaxel *in vivo*. Histological cross sections of H1975 tumor tissues excised from mice on day 1 postinjection of (A) paclitaxel, (B) PtSLNs, or (C) cetuxi-PtSLNs at an equivalent paclitaxel concentration of 22 mg of paclitaxel/kg. Oregon Green 488 paclitaxel was incorporated into the SLN formulations to investigate the cellular localization of paclitaxel. Cell nuclei were visualized with DAPI (blue fluorescence). Scale bar = 50 μ m.

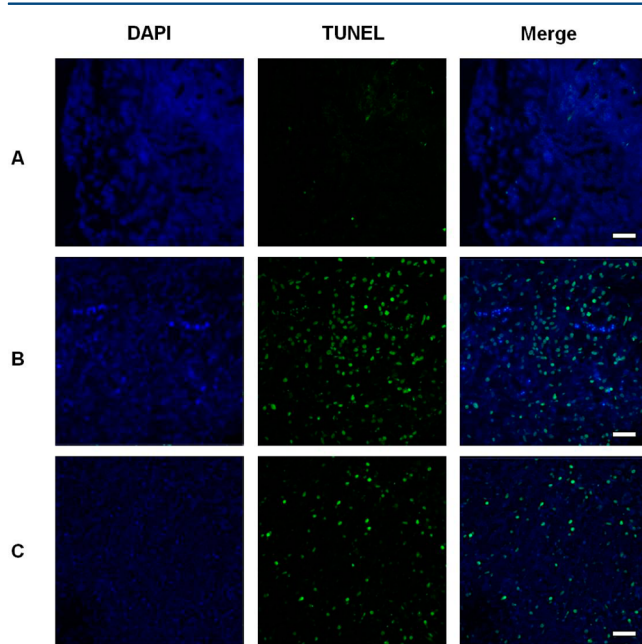


Figure 9. Detection of apoptosis *in vivo*. Histological cross sections of H1975 tumors tissues excised from the mice on day 1 postinjection of (A) Taxol and (B) cetuxi-PtSLNs and day 7 postinjection of (C) cetuxi-PtSLNs at an equivalent paclitaxel concentration of 22 mg of paclitaxel/kg. These sections were used to determine the extent of apoptosis with TUNEL assay. Cell nuclei were visualized with DAPI (blue fluorescence). Scale bar = 50 μ m.

agents in the form of nanoparticles yield maximum therapeutic potential.

Because of their excellent nanoscale reservoir structures for efficient encapsulation of therapeutics, high tumor targeting ability, and biosafety, tumor-targeting SLN formulations can potentially be used as delivery vehicles for other water-insoluble anticancer drugs, facilitating effective cancer therapy while reducing nonspecific side effects. In addition, by incorporating various active targeting ligands in the SLN complexes, these SLN complexes can be utilized as tumor-specific therapeutic carriers for treatment of various cancer types that overexpress well-characterized cell-surface proteins.

■ ASSOCIATED CONTENT

Supporting Information

Formulation compositions of SLNs, physicochemical properties of SLN formulations, characterization of antibody conjugation, time course changes of the hydrodynamic diameter of SLN formulations, targeted delivery of hercep-PtSLNs in cultured cancer cells, cell viability assay of SLN formulations, determination of the tolerable dose, determination of effective therapeutic dose, composition of tSLNs, physicochemical properties of SLN formulations, IC₅₀ values, pharmacokinetic parameters, and *in vivo* therapeutic parameters. This material is available free of charge via the Internet at <http://pubs.acs.org>.

■ AUTHOR INFORMATION

Corresponding Authors

*Tel: +82 2 3410 6459. Fax: +82 2 3410 0084. E-mail: hijunghee@skku.edu.

*Tel: +82 2 3410 3450. Fax: +82 2 3410 1754. E-mail: kpark@skku.edu.

Author Contributions

#These authors contributed equally to this work.

Notes

The authors declare no competing financial interest.

■ ACKNOWLEDGMENTS

This work was supported by a grant from the Korea Health Technology R&D Project, Ministry of Health & Welfare (A040041) of the Republic of Korea and the National Research Foundation (NRF) (2010-0029410) of the Republic of Korea. We thank Mijung Park for her help in establishing the synthetic compositions for SLNs, and Drs. Jong Mu Sun, Ji Hyun Lee, Jin Suk Ahn, Myung Ju Ahn, and Hyun Ryoung Kim for their comments and assistance. We also would like to express our sincere appreciation for the late Dr. Tae Gwan Park (Deceased, April 10, 2011) who was a constant source of inspiration and creative input.

■ REFERENCES

- (1) Ferrari, M. Nanotechnology-enabled medicine. *Discovery Med.* **2005**, *5*, 363–366.
- (2) Wang, A. Z.; Langer, R.; Farokhzad, O. C. Nanoparticle delivery of cancer drugs. *Annu. Rev. Med.* **2012**, *63*, 185–198.
- (3) Davis, M. E.; Zuckerman, J. E.; Choi, C. H.; Seligson, D.; Tolcher, A.; Alabi, C. A.; Yen, Y.; Heidel, J. D.; Ribas, A. Evidence of RNAi in humans from systemically administered siRNA via targeted nanoparticles. *Nature* **2010**, *464* (7291), 1067–1070.
- (4) Green, M. R.; Manikhas, G. M.; Orlov, S.; Afanasyev, B.; Makhson, A. M.; Bhar, P.; Hawkins, M. J. Abraxane, a novel Cremophor-free, albumin-bound particle form of paclitaxel for the treatment of advanced non-small-cell lung cancer. *Ann. Oncol.* **2006**, *17* (8), 1263–1268.

- (5) Yoo, J. W.; Irvine, D. J.; Discher, D. E.; Mitragotri, S. Bio-inspired, bioengineered and biomimetic drug delivery carriers. *Nat. Rev. Drug Discovery* **2011**, *10* (7), 521–535.
- (6) Jain, R. K.; Stylianopoulos, T. Delivering nanomedicine to solid tumors. *Nat. Rev. Clin. Oncol.* **2010**, *7* (11), 653–664.
- (7) Yi, S. W.; Yune, T. Y.; Kim, T. W.; Chung, H.; Choi, Y. W.; Kwon, I. C.; Lee, E. B.; Jeong, S. Y. A cationic lipid emulsion/DNA complex as a physically stable and serum-resistant gene delivery system. *Pharm. Res.* **2000**, *17* (3), 314–320.
- (8) Kim, Y. J.; Kim, T. W.; Chung, H.; Kwon, I. C.; Sung, H. C.; Jeong, S. Y. The effects of serum on the stability and the transfection activity of the cationic lipid emulsion with various oils. *Int. J. Pharm.* **2003**, *252* (1–2), 241–252.
- (9) Yoo, H. S.; Kwon, S. M.; Kim, Y. J.; Chung, H.; Kwon, I. C.; Kim, J.; Jeong, S. Y. Cationic lipid emulsions containing heavy oils for the transfection of adherent cells. *J. Controlled Release* **2004**, *98* (1), 179–188.
- (10) Deckelbaum, R. J.; Shipley, G. G.; Small, D. M. Structure and interactions of lipids in human plasma low density lipoproteins. *J. Biol. Chem.* **1977**, *252* (2), 744–754.
- (11) Prassl, R.; Pregetter, M.; Amenitsch, H.; Kriegbaum, M.; Schwarzenbacher, R.; Chapman, J. M.; Laggner, P. Low density lipoproteins as circulating fast temperature sensors. *PLoS One* **2008**, *3* (12), e4079.
- (12) Rowinsky, E. K. Clinical pharmacology of Taxol. *J. Natl. Cancer Inst. Monogr.* **1993**, No. 15, 25–37.
- (13) Weiss, R. B.; Donehower, R. C.; Wiernik, P. H.; Ohnuma, T.; Gralla, R. J.; Trump, D. L.; Baker, J. R., Jr.; Van Echo, D. A.; Von Hoff, D. D.; Leyland-Jones, B. Hypersensitivity reactions from taxol. *J. Clin. Oncol.* **1990**, *8* (7), 1263–1268.
- (14) Singla, A. K.; Garg, A.; Aggarwal, D. Paclitaxel and its formulations. *Int. J. Pharm.* **2002**, *235* (1–2), 179–192.
- (15) Gelderblom, H.; Verweij, J.; Nooter, K.; Sparreboom, A. Cremophor EL: the drawbacks and advantages of vehicle selection for drug formulation. *Eur. J. Cancer* **2001**, *37* (13), 1590–1598.
- (16) Kim, S. C.; Kim, D. W.; Shim, Y. H.; Bang, J. S.; Oh, H. S.; Wan Kim, S.; Seo, M. H. In vivo evaluation of polymeric micellar paclitaxel formulation: toxicity and efficacy. *J. Controlled Release* **2001**, *72* (1–3), 191–202.
- (17) Devalapally, H.; Chakilam, A.; Amiji, M. M. Role of nanotechnology in pharmaceutical product development. *J. Pharm. Sci.* **2007**, *96* (10), 2547–2565.
- (18) Wang, H.; Zhao, Y.; Wu, Y.; Hu, Y. L.; Nan, K.; Nie, G.; Chen, H. Enhanced anti-tumor efficacy by co-delivery of doxorubicin and paclitaxel with amphiphilic methoxy PEG-PLGA copolymer nanoparticles. *Biomaterials* **2011**, *32* (32), 8281–8290.
- (19) Cheng, J.; Teply, B. A.; Sherifi, I.; Sung, J.; Luther, G.; Gu, F. X.; Levy-Nissenbaum, E.; Radovic-Moreno, A. F.; Langer, R.; Farokhzad, O. C. Formulation of functionalized PLGA-PEG nanoparticles for in vivo targeted drug delivery. *Biomaterials* **2007**, *28* (5), 869–876.
- (20) Lee, A. L.; Wang, Y.; Cheng, H. Y.; Pervaiz, S.; Yang, Y. Y. The co-delivery of paclitaxel and Herceptin using cationic micellar nanoparticles. *Biomaterials* **2009**, *30* (5), 919–927.
- (21) Lee, K. S.; Chung, H. C.; Im, S. A.; Park, Y. H.; Kim, C. S.; Kim, S. B.; Rha, S. Y.; Lee, M. Y.; Ro, J. Multicenter phase II trial of Genexol-PM, a Cremophor-free, polymeric micelle formulation of paclitaxel, in patients with metastatic breast cancer. *Breast Cancer Res.* **2008**, *108* (2), 241–250.
- (22) Kato, K.; Chin, K.; Yoshikawa, T.; Yamaguchi, K.; Tsuji, Y.; Esaki, T.; Sakai, K.; Kimura, M.; Hamaguchi, T.; Shimada, Y.; Matsumura, Y.; Ikeda, R. Phase II study of NK105, a paclitaxel-incorporating micellar nanoparticle, for previously treated advanced or recurrent gastric cancer. *Invest. New Drugs* **2012**, *30* (4), 1621–1627.
- (23) Hrkach, J.; Von Hoff, D.; Mukkaram Ali, M.; Andrianova, E.; Auer, J.; Campbell, T.; De Witt, D.; Figa, M.; Figueiredo, M.; Horhota, A.; Low, S.; McDonnell, K.; Peeke, E.; Retnarajan, B.; Sabnis, A.; Schnipper, E.; Song, J. J.; Song, Y. H.; Summa, J.; Tompsett, D.; Troiano, G.; Van Geen Hoven, T.; Wright, J.; LoRusso, P.; Kantoff, P. W.; Bander, N. H.; Sweeney, C.; Farokhzad, O. C.; Langer, R.; Zale, S. Preclinical development and clinical translation of a PSMA-targeted docetaxel nanoparticle with a differentiated pharmacological profile. *Sci. Transl. Med.* **2012**, *4* (128), 128ra39.
- (24) Kim, H. R.; Kim, I. K.; Bae, K. H.; Lee, S. H.; Lee, Y.; Park, T. G. Cationic solid lipid nanoparticles reconstituted from low density lipoprotein components for delivery of siRNA. *Mol. Pharmaceutics* **2008**, *5* (4), 622–631.
- (25) Perrault, S. D.; Walkey, C.; Jennings, T.; Fischer, H. C.; Chan, W. C. Mediating tumor targeting efficiency of nanoparticles through design. *Nano Lett.* **2009**, *9* (5), 1909–1915.
- (26) Park, J. W.; Hong, K.; Kirpotin, D. B.; Colbern, G.; Shalaby, R.; Baselga, J.; Shao, Y.; Nielsen, U. B.; Marks, J. D.; Moore, D.; Papahadjopoulos, D.; Benz, C. C. Anti-HER2 immunoliposomes: enhanced efficacy attributable to targeted delivery. *Clin. Cancer Res.* **2002**, *8* (4), 1172–1181.
- (27) Kirpotin, D. B.; Drummond, D. C.; Shao, Y.; Shalaby, M. R.; Hong, K.; Nielsen, U. B.; Marks, J. D.; Benz, C. C.; Park, J. W. Antibody targeting of long-circulating lipidic nanoparticles does not increase tumor localization but does increase internalization in animal models. *Cancer Res.* **2006**, *66* (13), 6732–6740.
- (28) Bartlett, D. W.; Su, H.; Hildebrandt, I. J.; Weber, W. A.; Davis, M. E. Impact of tumor-specific targeting on the biodistribution and efficacy of siRNA nanoparticles measured by multimodality in vivo imaging. *Proc. Natl. Acad. Sci. U.S.A.* **2007**, *104* (39), 15549–15554.
- (29) Gianni, L.; Kearns, C. M.; Giani, A.; Capri, G.; Vigano, L.; Lacatelli, A.; Bonadonna, G.; Egorin, M. J. Nonlinear pharmacokinetics and metabolism of paclitaxel and its pharmacokinetic/pharmacodynamic relationships in humans. *J. Clin. Oncol.* **1995**, *13* (1), 180–190.